

Whole-Heart Free-Breathing Phase-Sensitive Inversion-Recovery Late Gadolinium Enhancement Imaging with High Isotropic Spatial Resolution Using Respiratory Self-Navigation: a First Patient Study

Davide Piccini^{1,2}, Simone Coppo², Giulia Ginami², Gabriele Bonanno², Tobias Rutz³, Gabriella Vincenti³, Jürg Schwitter³, and Matthias Stuber²

¹Advanced Clinical Imaging Technology, Siemens Healthcare IM BM PI, Lausanne, Switzerland, ²Department of Radiology, University Hospital (CHUV) and University of Lausanne (UNIL) / Center for Biomedical Imaging (CIBM), Lausanne, Switzerland, ³Division of Cardiology and Cardiac MR Center, University Hospital of Lausanne (CHUV), Lausanne, Switzerland

TARGET AUDIENCE: Scientists and clinicians interested in myocardial fibrosis and EP procedures.

PURPOSE: With the introduction of respiratory self-navigation (SN) [1], the acquisition of whole heart coronary MR angiography (MRA) datasets with high isotropic spatial resolution can be achieved during free-breathing without the need for respiratory navigators [2]. SN, in combination with a 3D radial trajectory [1,3] has successfully been tested for the acquisition of non-contrast and post-contrast whole-heart coronary MRA in both volunteers [3] and patients [4]. However, the clinical utility of an easy-to-acquire, dataset with high isotropic resolution and broad anatomical coverage can be expanded to several other cardiac applications. In particular, its robustness to motion and undersampling has not yet been fully exploited for the complete anatomical characterization of myocardial scar tissue in 3D. For these reasons, a phase-sensitive inversion recovery (PSIR) acquisition and reconstruction [5] technique was developed on the base of an existing 3D radial SN imaging sequence [4]. The modified sequence (3D-SN PSIR) was tested using late gadolinium enhanced (LGE) imaging in patients with established coronary artery disease (CAD) and positive LGE findings observed in conventional 2D PSIR acquisitions.

METHODS: A previously published prototype version of a 3D radial SN bSSFP whole-heart sequence and reconstruction algorithm [3] was adapted to perform a PSIR-like acquisition as described in [5]. The acquisition was ECG triggered and segmented over two successive heartbeats. A non-volume-selective inversion recovery (IR) pulse was applied every first heartbeat, followed by a bSSFP acquisition segment. The second heartbeat was then used to acquire the corresponding segment of the reference phase volume, with a lower radio frequency (RF) excitation angle. The same radial readouts were encoded in the two segments of the two heartbeats as shown in the sequence diagram in Fig.1. The two images (IR and reference) were then separately regridded, while respiratory motion correction was performed using the algorithm described in [6] to be able to correct and co-register both acquisitions to the same respiratory position. After regridding, the two complex 3D volumes were combined, slice by slice, using the algorithm described in [5], to obtain both a simple magnitude IR volume (3D-SN IR) and a PSIR volume. In-vivo exams were performed on a 1.5T clinical MRI scanner (MAGNETOM Aera, Siemens AG, Erlangen, Germany). Patients (n=7) with positive findings on the conventional multi-breathhold 2D PSIR identified during clinical routine contrast enhanced (total of 0.2 mmol/kg of Gadobutrol; Gadovist, Bayer Schering Pharma, Zurich, Switzerland) cardiac MRI underwent the research 3D SN PSIR protocol at the end of the regular scan session. Data acquisition was performed during the most quiescent diastolic phase with the segmented, ECG-triggered, fat-saturated, 3D-SN PSIR imaging sequence. Parameters were: TR/TE 2.9/1.45ms, FOV (220mm)³, matrix 160³, voxel size (1.4mm)³, RF excitation angle 115° and 8° (IR and reference segments respectively), and receiver bandwidth 895Hz/Px. The inversion time (TI) of the 3D-SN PSIR acquisitions was always identical to that of the preceding 2D PSIR acquisition, ranging between 250-320ms. A total of about 8100 radial readouts were acquired over (300x2) heartbeats for each 3D scan during free breathing with 100% respiratory efficiency. The conventional 2D PSIR acquisitions, conversely, were gradient echo based and acquired in systole, with parameters: TR/TE 6.3/3.2ms, FOV (~200x380)mm², matrix 156x256, voxel size (~2.0x1.5)mm², slice thickness 8mm, RF excitation angle 25° and 8°, and bandwidth 140Hz/Px. 3D-SN IR and 3D-SN PSIR datasets were visually compared, while 2D PSIR and 3D-SN PSIR patient datasets were compared for acquisition time, and LGE findings. All datasets were graded by two experienced cardiologists on a scale from 4 (very good) to 1 (non-diagnostic), where 3 and 2 indicate moderate and severe blurring.

RESULTS: Self-navigation was successful in all 3D-SN PSIR acquisitions. The average acquisition time for the patient datasets was 13.3±5.2min for the 2D and 8.5±1.3min for the 3D acquisitions (p<0.05). A complete diagnosis on the LGE findings could be reached in 7/7 patients with the 2D approach, and in 6/7 patients with 3D-SN PSIR. The average grade of the 3D-SN PSIR was 3.0±1.1 (all grades 4 in 2D). A complete analysis of all patients included in this study is reported in Tab 1. The 3D-SN dataset of patient 4, with LGE findings in the descending aorta (green arrow), is displayed in Fig.2 showing how the 3D-SN PSIR always achieved an effective nulling of the healthy myocardium signal in comparison to the magnitude IR dataset, even when TI was suboptimal (red arrows). An example comparing the same LGE findings in 2D PSIR (8mm slice thickness / systolic) and 3D-SN PSIR datasets (1.4mm isotropic resolution / diastolic) is shown (Fig.3).

DISCUSSION AND CONCLUSIONS: These preliminary results show that the proposed technique might offer a promising, easy to use, and more time effective alternative to standard breathhold 2D PSIR LGE imaging. The image quality of the 3D-SN PSIR datasets enabled a complete diagnosis in almost all cases, while the low image quality in one patient (with grade 1) was probably linked to the increased delay time between contrast injection and 3D data acquisition, caused by a lengthy (>22min) 2D acquisition. Therefore, it may be hypothesized that the contrast agent concentration may no longer have been optimal. Future experiments will be performed acquiring conventional 2D-PSIR and 3D-SN-PSIR data in two separate sessions in order to assure identical timing of acquisitions after contrast agent injection. The possibility to easily acquire 3D high-resolution LGE datasets may further represent an important step towards planning of MRI-guided electrophysiology procedures.

REFERENCES: [1] Stehning C, MRM 2005; [2] Ehman RL, Radiol 1989; [3] Piccini D, MRM 2012; [4] Piccini D, Radiol 2014; [5] Kellman P, MRM 2002; [6] Ginami G, ISMRM 2014.

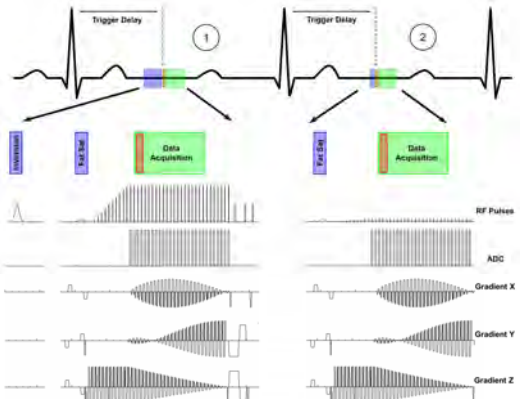


Fig. 1: Acquisition scheme of the 3D-SN PSIR sequence. 3D radial data acquisition is ECG triggered and segmented. (1) In the first heartbeat an IR pulse is applied, followed by a bSSFP acquisition, while (2) in the second heartbeat the same segment is acquired with a much lower RF excitation angle (reference).

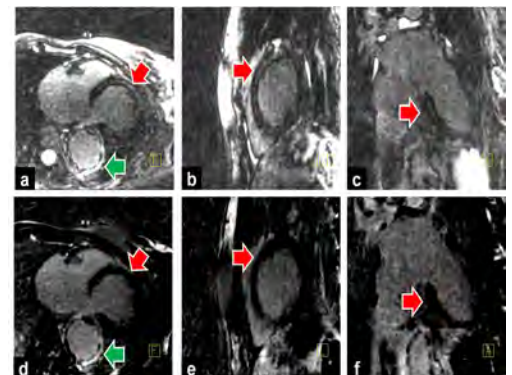


Fig. 2: Comparison between 3D-SN IR (a-TRA, b-SAG, and c-COR) and 3D-SN PSIR (d,e,f) volumes in patient 4, with LGE findings in the descending aorta (green). As the TI was not optimal, the healthy myocardium in the IR volume was not completely nulled, while nulling was highly effective for the 3D-SN PSIR volume (red arrows).

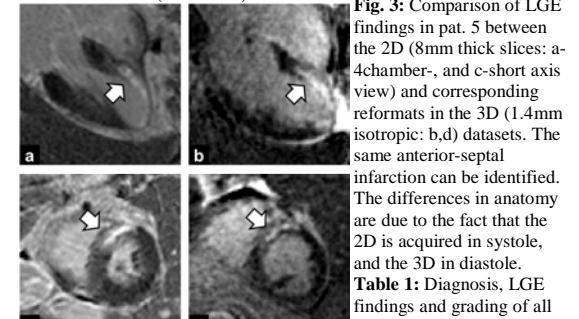


Fig. 3: Comparison of LGE findings in pat. 5 between the 2D (8mm thick slices: a-4chamber, b-c-short axis view) and corresponding reformats in the 3D (1.4mm isotropic: b,d) datasets. The same anterior-septal infarction can be identified. The differences in anatomy are due to the fact that the 2D is acquired in systole, and the 3D in diastole.

Table 1: Diagnosis, LGE findings and grading of all n=7 patients.

Patient Diagnosis	LGE finding	Diagnosis 2D PSIR	Diagnosis 3D-SN PSIR
1 Constrictive pericarditis	LGE of pericardium.	Complete Grade 4	Complete Grade 3
2 Inferior myocardial infarction	LGE of basal and mid segments of the inferior-septal and inferior wall.	Complete Grade 4	Complete Grade 3
3 Anterior myocardial infarction	LGE + microvascular obstruction in septal wall. LGE + no microvascular obstruction in basal anterior, inferior, apex, inferior-apical, lateral-apical and anterolateral segments.	Complete Grade 4	Complete Grade 4
4 Dissection of desc. aorta, replacement and stenting	No myocardial LGE. LGE in descending thoracic and abdominal aorta. Stent in type B dissection.	Not performed	Complete Grade 4
5 Anterior myocardial infarction	LGE of anterior-septal wall , apical segments of anterior, septal and inferior wall.	Complete Grade 4	Complete Grade 4
6 Anterior and antero-septal infarction	LGE in anterior, apical, and anterior-septal wall, inferior and lateral-apical wall.	Complete Grade 4	Partial Grade 1
7 Infero-lateral myocardial infarction	LGE in inferior-lateral wall	Complete Grade 4	Complete Grade 2